Original Article

pISSN 2234-7518 • eISSN 2005-372X
https://doi.org/10.4041/kjod.2017.47.1.3

THE KOREAN JOURNAL of ORTHODONTICS
KJO

Incorporation of silver nanoparticles on the surface of orthodontic microimplants to achieve antimicrobial properties

Adith Venugopal[a]
Nallal Muthuchamy[b]
Harsh Tejani[a]
Anantha-Iyengar-Gopalan[c,d]
Kwang-Pill Lee[b,c,d]
Heon-Jin Lee[e]
Hee Moon Kyung[a]

[a]Department of Orthodontics, School of Dentistry, Kyungpook National University, Daegu, Korea
[b]Department of Chemistry Education, Kyungpook National University, Daegu, Korea
[c]Research Institute of Advanced Energy Technology, Kyungpook National University, Daegu, Korea
[d]Department of Nanoscience and Nanotechnology, Kyungpook National University, Daegu, Korea
[e]Department of Oral Microbiology and Immunology, Kyungpook National University, Daegu, Korea

Objective: Microbial aggregation around dental implants can lead to loss/loosening of the implants. This study was aimed at surface treating titanium microimplants with silver nanoparticles (AgNPs) to achieve antibacterial properties. **Methods:** AgNP-modified titanium microimplants (Ti-nAg) were prepared using two methods. The first method involved coating the microimplants with regular AgNPs (Ti-AgNP) and the second involved coating them with a AgNP-coated biopolymer (Ti-BP-AgNP). The topologies, microstructures, and chemical compositions of the surfaces of the Ti-nAg were characterized by scanning electron microscopy (SEM) equipped with energy-dispersive spectrometer (EDS) and X-ray photoelectron spectroscopy (XPS). Disk diffusion tests using *Streptococcus mutans*, *Streptococcus sanguinis*, and *Aggregatibacter actinomycetemcomitans* were performed to test the antibacterial activity of the Ti-nAg microimplants. **Results:** SEM revealed that only a meager amount of AgNPs was sparsely deposited on the Ti-AgNP surface with the first method, while a layer of AgNP-coated biopolymer extended along the Ti-BP-AgNP surface in the second method. The diameters of the coated nanoparticles were in the range of 10 to 30 nm. EDS revealed 1.05 atomic % of Ag on the surface of the Ti-AgNP and an astounding 21.2 atomic % on the surface of the Ti-BP-AgNP. XPS confirmed the metallic state of silver on the Ti-BP-AgNP surface. After 24 hours of incubation, clear zones of inhibition were seen around the Ti-BP-AgNP microimplants in all three test bacterial culture plates, whereas no antibacterial effect was observed with the Ti-AgNP microimplants. **Conclusions:** Titanium microimplants modified with Ti-BP-AgNP exhibit excellent antibacterial properties, making them a promising implantable biomaterial.
[Korean J Orthod 2017;47(1):3-10]

Key words: Nanosilver, Microimplant, Antimicrobial

Received February 25, 2016; Revised May 14, 2016; Accepted June 21, 2016.

Corresponding author: Hee Moon Kyung.
Professor, Department of Orthodontics, School of Dentistry, Kyungpook National University, 2177 Dalgubeoldae-ro, Jung-gu, Daegu 41940, Korea.
Tel +82-53-600-7372 **e-mail** hmkyung@knu.ac.kr

The authors report no commercial, proprietary, or financial interest in the products or companies described in this article.

INTRODUCTION

Orthodontic microimplants are manufactured from materials such as commercially pure titanium, surgical stainless steel, and titanium alloys (Ti6Al4V). Titanium alloy offers enhanced tissue compatibility, corrosion resistance, bacteriostatic action, and mechanical strength compared to stainless steel. These enhanced features of titanium alloys may be attributed to the titanium dioxide (TiO_2) film that forms on the surface of the alloys.[1]

Several factors including osseointegration at the bone-implant interface and the amount of bacterial colonization around the implants influence the final characteristics and outcomes of dental and orthodontic microimplants.[2] According to previous studies, the long term survival or stability of implants primarily depends on the inflammatory condition that causes peri-implantitis and loss of supporting bone.[3] Inflammation leads to progressively escalating damage to the cortical bone, especially around the neck of the implants.[4,5] Peri-implant mucositis, an inflammatory lesion, not only affects the soft tissues but also damages the supporting bone.[6] According to a previous study, 43% of individuals with implants suffer from peri-implantitis, and peri-implant mucositis was seen in up to 50% of the cases.[7] Thus, limiting the amount of inflammation is vital for ensuring long term stability and success of the implant.
Infection of the implants and their subsequent loosening is most commonly seen in titanium-based prosthesis and can largely be avoided by inhibiting the adhesion of microbes on the surface of the implanted devices.[8] The initial colonizers that adhere to tooth and implant surfaces include *Streptococcus oralis*, *Streptococcus sanguinis*, and *Streptococcus mutans*. In addition, *Aggregatibacter actinomycetemcomitans*, a gram-negative bacterium, is also essentially known to be responsible for many periodontal and peri-implant diseases.[9]

Many methods including surface treatments such as polishing and modification of surface free energy[10-13] have been employed to reduce or nullify the bacterial aggregation around titanium-based prosthesis. Elemental silver has been specifically known for its array of antimicrobial properties for many years.[14] Many previous studies have demonstrated the excellent antibacterial properties of silver-impregnated hydroxyl apatite films as well as silver zeolite against different cultured bacteria.[15-17] It has been speculated that several mechanisms are involved in the antibacterial potency of nanosilver. Due to an extraordinarily large surface area, silver nanoparticles (AgNPs) exhibit better antibacterial properties than metallic silver.[18] Therefore, in the recent past, the amalgamation of AgNPs with different biomaterials to improve the biocompatibility and antibacterial capability has been intensely studied, and many incorporations such as silver-doped hydroxyl apatite, polymer AgNPs, and AgNPs on TiO_2 have been developed.[19-21]

In light of the above findings, in this study, we aimed at preparing AgNP-modified titanium microimplants (Ti-nAg) using two methods. Further, we determined the size, morphology, and distribution of the AgNPs and examined and compared the antibacterial properties of the modified microimplants using a well-established microbiological assay.

MATERIALS AND METHODS

The microimplants were divided into three groups of forty titanium alloy (Ti6Al4V) microimplants (Absoanchor®; Dentos, Daegu, Korea) based on the method of AgNP deposition: a) regular AgNP deposition, Ti-AgNP group; b) AgNP-coated biopolymer deposition, Ti-BP-AgNP group; c) control group (no deposition).

Fabrication of the Ti-BP-AgNP implant

This novel process involved three stages: i) preparation of the hydroxyapatite/chitosan biopolymer; ii) biopolymer layer formation over the Ti6Al4V microimplant surface; and iii) deposition of the AgNPs on the titanium-biopolymer coating to form Ti-BP-AgNP.

i) Preparation of the hydroxyapetite/chitosan biopolymer

Triethylphosphite (98%; Sigma Aldrich, St. Louis, MO, USA) and calcium nitrate tetrahydrate (≥ 99%; Fluka, Seoul, Korea) were used as precursors in the preparation of crystalline hydroxyapatite. A Ca/P molar ratio of 1.6 was achieved by making aqueous solutions of each precursor. The phosphorous solution was added drop wise to the calcium solution under vigorous stirring while maintaining the temperature at 65°C and the pH at 8. NH_4OH (28% w/w; Fluka) aqueous solution was used to control the pH. The colloidal solution prepared was continuously stirred at 65°C for 2 hours and then aged at 25°C for 24 hours to obtain a white and viscous gel. The gel was then dried in a vacuum chamber at 100°C until the solvent was completely removed. The dry powder was then ground and calcined at 550°C for 2 hours till a well-crystallized hydroxyapatite (HA) powder was obtained.[22]

Chitosan and acetic acid were obtained from Sigma-Aldrich. Isopropyl alcohol (Duksan Pure Chemicals Co., Ltd., Ansan, Korea), oxalic acid (Shinyo Pure Chemical Co., Osaka, Japan), and silver nitrate (Kojima Chemicals, Sayama, Japan) were used as received.

Aqueous chitosan (biopolymer) solution (2 wt%

https://doi.org/10.4041/kjod.2017.47.1.3

solution) containing a compatibilizer polymer and crosslinker was prepared by dissolving chitosan granules in 5% acetic acid at a temperature of 60°C under continuous stirring. The crystallized HA powder was then added to the chitosan preparation and stirred at room temperature using a magnetic stirrer. The solution was continuously stirred for another 24 hours until a homogenous polymer mix was obtained, after which the solution was cooled to room temperature.

ii) Biopolymer layer formation over the Ti6Al4V microimplant surface

Pristine titanium microimplants were rinsed by ultrasonic radiation in ethanol and dried. The TI6Al4V microimplants were then dropped into the biopolymer solution (HA/chitosan) and stirred continuously for six hours. The biopolymer coated titanium microimplants were then filtered out and dried at 60°C for further deposition with the AgNPs. During the drying process, the biopolymer layer adhered on to the titanium microimplant surface.

iii) Deposition of the AgNPs on the titanium-biopolymer coating to form Ti-BP-AgNP

AgNPs were deposited onto the biopolymer-coated titanium microimplants via photoreduction of Ag ions. The biopolymer-coated microimplants were then immersed in a 2 mM aqueous solution of silver nitrate in isopropyl alcohol, which functioned as the reducing agent for the Ag ions. The biopolymer-coated microimplants containing the solution were irradiated with ultraviolet light (365 nm) for a defined period (30 minutes). After deposition of the AgNPs over the biopolymer-coated titanium microimplants, the microimplants were rinsed in distilled water and dried in a microwave.

The group designated as Ti-AgNP (titanium implants with regular deposition of AgNPs) were prepared using the above-mentioned method alone without the addition of the biopolymer composite layer.

Characterization of the surface coating on the titanium microimplant

Scanning electron microscopy (SEM; HITACHI S-4500, Hitachi, Tokyo, Japan) with an energy-dispersive spectrometer (EDS) was used to assess and visualize the surface morphology of the microimplants. The samples were sputtered with a platinum layer to increase the conductivity. The surface elemental compositions were characterized by X-ray photoelectron spectroscopy (XPS; Kratos Axis Ultra spectrometer, Surface Science, Manchester, UK) using Al Kα (E = 1486.6 eV). The deposited surface was etched by Ar ion sputtering at energy of 4 keV for 5 minutes to analyze the chemical state of the Ti-BP-AgNP microimplants. Survey scan analyses for an area of 300 × 700 μm were performed.

Antibacterial tests

Gram-positive bacteria, *Streptococcus* sp., and gram-negative *A. actinomycetemcomitans* were used to test the antibacterial activity of the surfaces of the two types of Ti-nAg microimplants. Disc diffusion tests were performed to determine the zone of inhibition in millimeters, thereby gauging the magnitude of silver ions released from the Ti-nAg surface. Brain heart infusion (BHI) agar plates were used to evaluate the antibacterial

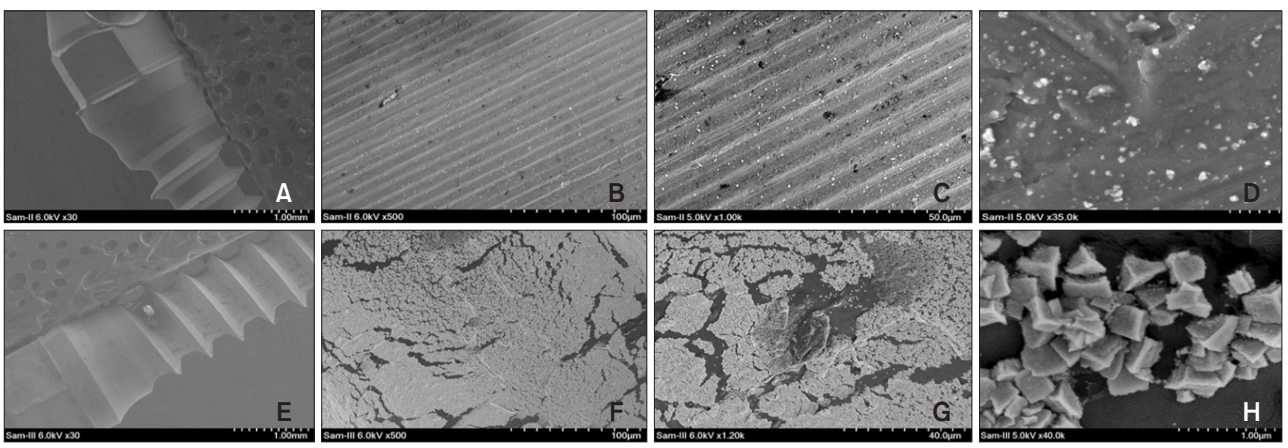

Figure 1. Surface characterization of the Ti-nAg microimplants. scanning electron micrographs show Ti-AgNP surface at different magnifications. **A**, 30×; **B**, 500×; **C**, 1,000×; and **D**, 35,000×. And Ti-BP-AgNP surface at **E**, 30×; **F**, 500×; **G**, 12,000×; and **H**, 40,000× magnifications.
Ti-AgNP, Microimplant coated with regular silver nanoparticles (AgNPs); Ti-BP-AgNP, microimplant coated with biopolymer-AgNP.

 https://doi.org/10.4041/kjod.2017.47.1.3

activity of the microimplants. These tests conformed to the recommended standards of the National Committee for Clinical Laboratory Standards (NCCLS; now renamed as Clinical and Laboratory Standards Institute, CLSI, 2000). *S. mutans* ATCC®25175™, *S. sanguinis* ATCC®10556™, and *A. actinomycetemcometans* ATCC®33384™ (Koram Biotech Corp., Seoul, Korea) were used for the antibacterial effect assay.

Saline suspensions of isolated colonies selected from the BHI agar plates were used to prepare the bacterial suspensions. The BHI plates were then cultured for the next 24 hours. The suspension was adjusted to match the tube of 0.5 McFarland turbidity standard using a spectrophotometer at 600 nm, which equaled to 1.5×10^8 colony-forming units (CFU)/mL. A sterile swab completely steeped in the prepared bacterial suspension was used to inoculate the surface of the BHI plates. Finally, the test microimplants were placed on the inoculated agar plate and incubated at 37°C for 24 hours. After incubation, the length, breadth, and area of the inhibition zones were measured and tabulated. All the tests were performed in triplicate.

RESULTS

SEM images of the microimplants with regular AgNP deposition and BP-AgNP deposition are shown in Figure 1. Even though all the samples were sintered at an even temperature, the structure of the established crystal grains seemed to vary based on the silver content and concentration. Because heavy elements (e.g., Ag) backscatter electrons more strongly than light elements (e.g., O, Ti), the metallic silver appears brighter. The Ti-AgNP microimplants showed shining AgNPs with a diameter of around 30 nm, which were well scattered as shown in Figure 1B, 1C, and 1D. Many of the scattered AgNPs elicited an amorphous structure and formed agglomerates (Figure 1D). On the other hand, the microimplants deposited with BP-AgNP displayed a more rough surface morphology. The addition of a biopolymer

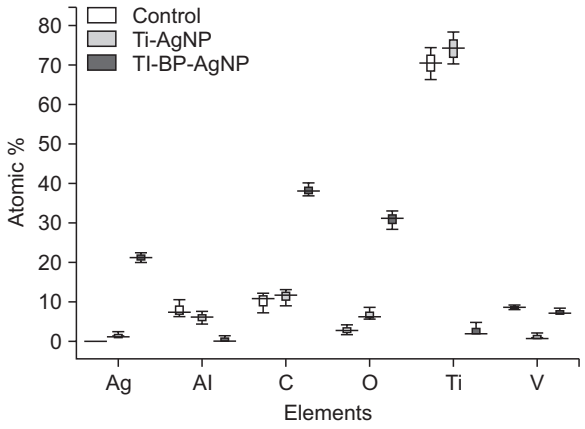

Figure 2. Energy-dispersive spectroscopy plots of the elements on the control, Ti-AgNP, and Ti-BP-AgNP microimplants.
Ti-AgNP, Microimplant coated with regular silver nanoparticles (AgNPs); Ti-BP-AgNP, microimplant coated with biopolymer-AgNP.

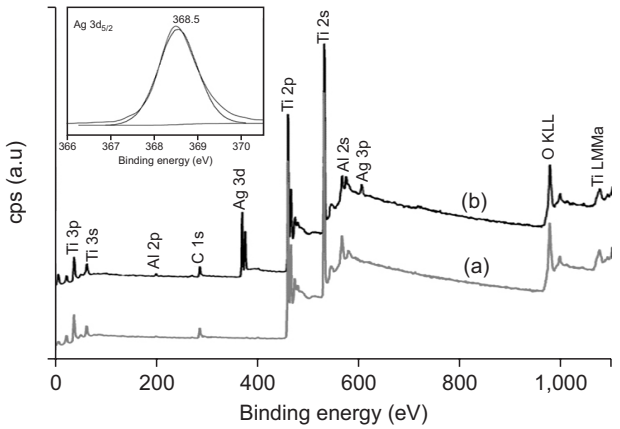

Figure 3. Left: X-ray photoelectron spectroscopy (XPS) spectra of (a) control (no deposition) and (b) BP-AgNP-coated microimplants. Right: High-resolution XPS spectra of Ag $3d_{5/2}$ in the BP-AgNP coated microimplants.
BP-AgNP, Biopolymer-silver nanoparticles.

Table 1. Composition of the control, Ti-AgNP, and Ti-BP-AgNP microimplants, as determined using energy-dispersive spectroscopy

Sample	Atomic %					
	Ti	Al	V	C	O	Ag
Control (no deposition)	70.4	7.3	8.5	10.8	2.7	–
Ti-AgNP	74.3	6.1	0.70	11.8	6.1	1.05
Ti-BP-AgNP	1.74	0.37	7.09	38.11	31.3	21.2

Ti-AgNP, Microimplant coated with regular silver nanoparticles (AgNPs); Ti-BP-AgNP, microimplant coated with biopolymer-AgNP.

https://doi.org/10.4041/kjod.2017.47.1.3

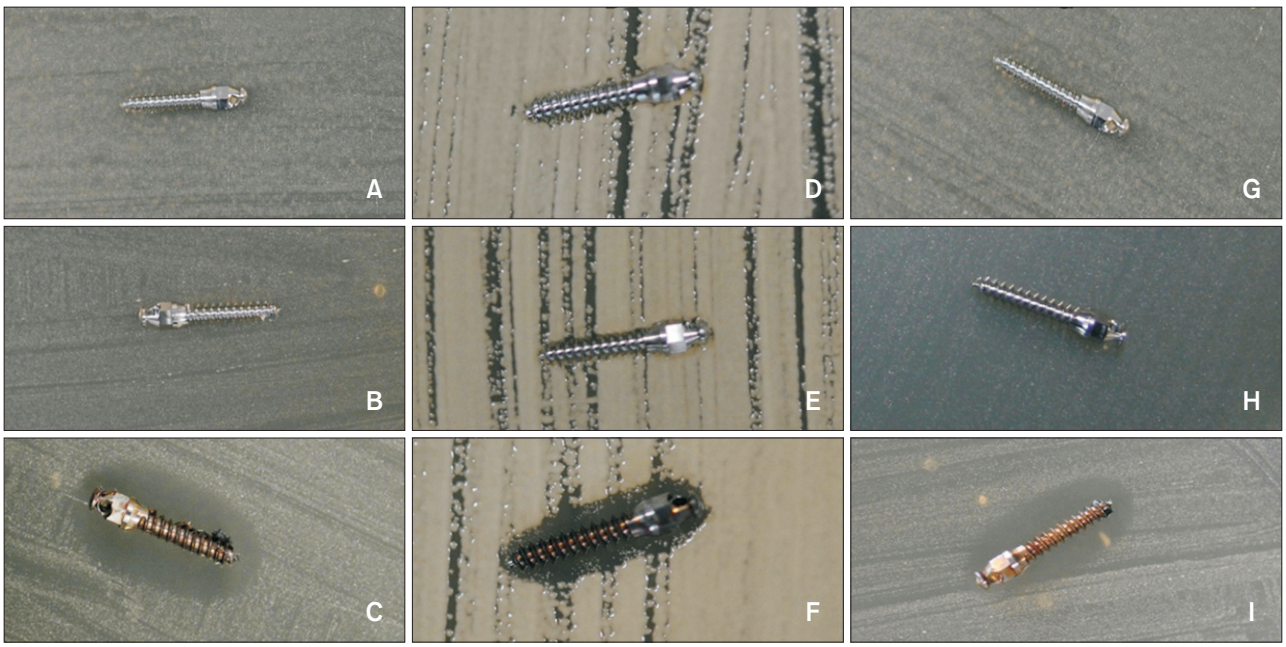

Figure 4. Disk diffusion tests showing zone of inhibition for (**A**) *Streptococcus mutans* with the control microimplant; (**B**) *S. mutans* with Ti-AgNP; (**C**) *S. mutans* with Ti-BP-AgNP; (**D**) Aggregatibacter actinomycetemcometans with the control microimplant; (**E**) *A. actinomycetemcometans* with Ti-AgNP; (**F**) *A. actinomycetemcometans* with Ti-BP-AgNP; (**G**) *S. sanguinis* with the control microimplant; (**H**) *S. sanguinis* with Ti-AgNP; and (**I**) *S. sanguinis* with Ti-BP-AgNP.
ZOI, Zone of inhibition; Ti-AgNP, microimplant coated with regular silver nanoparticles (AgNPs); Ti-BP-AgNP, microimplant coated with biopolymer-AgNP.

Table 2. Length, breadth, and area of the zone of inhibition (ZOI) as seen with the control and test titanium microimplants (Ti-AgNP and Ti-BP-AgNP) on three different bacterial culture plates

Bacteria	ZOI								
	Ti-AgNP			Ti-BP-AgNP			Control		
	l	b	Area	l	b	Area	l	b	Area
Streptococcus mutans	–	–	–	11.18 ± 0.53	5.75 ± 0.37	50.58 ± 4.88	–	–	–
Streptococcus sanguinis	–	–	–	9.62 ± 0.44	3.68 ± 0.25	27.93 ± 3.01	–	–	–
Aggregatibacter actinomycetemcomitans	–	–	–	9.50 ± 0.46	3.37 ± 0.44	25.13 ± 3.06	–	–	–

Values are presented as mean ± standard deviation.
Ti-AgNP, Microimplant coated with regular silver nanoparticles (AgNPs); Ti-BP-AgNP, microimplant coated with biopolymer-AgNP; l, length; b, breadth; –, not appeared.
Due to linear samples, the ZOI was measured in terms of length (mm), breadth (mm), and area (mm^2). Area of the ellipse was measured as π (l/2 × b/2).

layer resulted in a combination of mesoporous and macroporous surface matrix (Figure 1F), including AgNPs (shiny dots) of varying diameters ranging from 10 to 30 nm (Figure 1H).

EDS spectra plots of the Ti-BP-AgNP microimplants showed the presence of a higher peak for atomic silver deposited within the surface compared to that of the Ti-AgNP microimplant (Figure 2). Quantification of the spectra indicated that the Ti-AgNP microimplant surface contained only 1.05 atomic % of silver. On the other hand, the spectra for the TI-BP-AgNP surface showed an astounding silver atomic % of 21.2 (Table 1).

The BP-AgNP coated microimplants were further characterized by XPS measurements to identify and assess the chemical state of silver. Figure 3 shows the XPS profiles of the control (red, a) and Ti-BP-AgNP microimplants (black, b). The peak for elemental silver can be visualized on the surface of the coated microimplant. The XPS spectra of Ag $3d_{5/2}$ from the microimplant right after the deposition was registered,

 https://doi.org/10.4041/kjod.2017.47.1.3

as this electronic configuration of Ag specifically demonstrated the reactive sub shell that was responsible for its reactivity and chemical interactions. The Ag $3d_{5/2}$ peak appeared at a binding energy of 368.5 eV, suggesting that the silver was of metallic nature (Figure 3).[23]

The antibacterial activity of the microimplants was confirmed by the presence of an inhibition zone of the growth of *S. mutans*, *S. sanguinis*, and *A. actinomycetemcometans* around the substrates as shown in Figure 4. No bacterial growth was observed around the Ti-BP-AgNP microimplants (Figure 4C, 4F, and 4I). However, bacterial growth was detected around both the control as well as the Ti-AgNP microimplants. Table 2 illustrates the zone of inhibition measurements of the test samples for quantitative assessment. The area of the zone of inhibition for *S. mutans* (50.58 ± 4.88 mm^2) was the largest with Ti-BP-AgNP microimplants, followed by that of *S. sanguinis* (27 ± 3.01 mm^2); the smallest zone of inhibition was observed for *A. actinomycetemcometans* (25 ± 3.06 mm^2). The Ti-AgNPs and the control microimplants showed no antibacterial effect on any of the three test bacteria (Table 2).

DISCUSSION

Incorporation of AgNps with different biomaterials to improve their antimicrobial characteristics is presently being studied extensively. In the current study, two methods were used to deposit AgNPs on the surface of titanium microimplants. One group was coated with regular AgNPs (Ti-AgNP), whereas the other was coated with BP-AgNP (Ti-BP-AgNP). After completion of the BP-AgNP deposition on the microimplant surface, the color of the microimplant had turned brownish-gold (Figure 4C, 4F, and 4I). No such color change was observed on the microimplants deposited with regular AgNPs. The SEM images showed AgNps sparsely dispersed over the Ti-AgNP microimplant surface with a diameter of approximately 30 nm, and many AgNPs formed agglomerates or clumps (Figure 1D). On the contrary, the Ti-BP-AgNP microimplants showed a disperse coating of the biopolymer of varying thickness all along the surface (Figure 1E) and exhibited a mesoporous/macroporous surface matrix with a pore diameter of roughly 40 to 50 nm (Figure 1G). On the surface of the biopolymer, AgNPs of different diameters ranging from 10 to 30 nm could be visualized (Figure 1H).

To verify the array of chemical elements and the elemental state of the AgNps, EDS and XPS analyses were performed. The EDS microanalyses confirmed that the atomic % of AgNps on the Ti-AgNP microimplants was merely 1.05%, whereas that on the surface of the Ti-BP-AgNP microimplants was 21.2% (Figure 2, Table 1). As the EDS analysis depended on a limited area for screening, the BP-AgNP layer covering the Ti surface caused a reduction in the values of the underlying elements Ti, Al, and V (Table 1). According to the XPS, the Ag3d region had well-separated spin-orbit components. This electronic configuration of Ag was specifically recorded as it demonstrated the reactive sub shell or the valence shell that is responsible for the high reactivity and surface interactions of the AgNps. The binding energy of the Ag $3d_{5/2}$ peak appeared at 368.5 eV, suggesting that the Ag was of metallic nature (Figure 3).[23]

A lot of speculation revolves around the antibacterial mechanism of AgNPs. Many theories explaining this phenomenon are linked to the ability of these nanoparticles to release ionic silver in an aqueous solution[24,25]; some are linked to their ability to react with the bacterial cell membrane and others are related to their potential to produce reactive oxygen species.[26] Most importantly, AgNPs are known to elicit antimicrobial properties due to their large surface area, which in turn provides for larger area for microbial contact. Some studies also suggest that silver ions have a strong affinity for the electron donor groups present in various sulfur-, oxygen-, or nitrogen-containing bacterial cells.[27]

Streptococcus sp. and *A. actinomycetemcomitans*, being the most common pathogens in the oral bio flora,[28] were considered appropriate for performing the antibacterial tests for the two different Ti-nAg surfaces in this study. We used the disk diffusion technique to determine the antibacterial properties of the Ti-nAg surfaces. No zone of inhibition was observed around the control and Ti-AgNP microimplants (Figure 4A, 4B, and 4D–4H), but the Ti-BP-AgNP microimplants exhibited excellent antibacterial effects with clear zones of inhibition in all three test bacterial culture plates (Figure 4C, 4F, and 4I). Our zone of inhibition tests depended on the amount or concentration of ionic silver leached from the surface of the test microimplants. Moreover, elemental silver has a low rate of dissolution in an aqueous environment. Therefore, it can be said that the Ti-BP-AgNP microimplants may have reached sufficient concentrations of ionic silver to demonstrate a clear zone, whereas the Ti-AgNP microimplants may not have reached a concentration sufficient to establish a clear zone. SEM and EDS examination also revealed that the Ti-AgNP microimplants had only a tiny percentage of silver deposited on their surface, which amounted to just 1.05 atomic %. Nanosilver is highly reactive and readily reacts with surface oxygen to form oxides, which reduces the available free nanosilver for interaction and thus decreases the antimicrobial properties[29]; accordingly, we

https://doi.org/10.4041/kjod.2017.47.1.3

believe that the high concentration of silver accounting for about 21.2 atomic % of AgNPs on the biopolymer layer in the Ti-BP-AgNP microimplant surface may have been the reason for its excellent antibacterial properties.

Polymers have a synergistic effect on nanosilver with regard to the bactericidal properties when they are used in combination, although the antibacterial efficiency of polymers alone is much weaker than that of nanosilver.[30,31] Therefore, biopolymers may stabilize and dispel nanosilver, thus preventing its oxidation and thereby increasing its bioavailability for enhancing its antibacterial properties. Nanosilver, with its substantial antibacterial properties, plays a pivotal role in the immediate antibacterial effect of nanosilver-deposited biopolymer coatings, where after the depletion of the silver ions, the biopolymer can have a firm effect on the permanent antibacterial effect of the coating.[32,33]

A thorough literature search in the medical database suggests that this is the first study reporting a novel method of fabrication of a biocompatible polymer coated with AgNPs on a titanium alloy microimplant surface and its comparison to regular AgNP deposition on a titanium alloy microimplant to understand the differences in the morphological structure and antimicrobial properties of the implants caused by the difference in the surface modification technique. Future studies on the sustainability of ion release from these nanoparticle-coated biopolymers, changes in the physical properties of the incorporated material, such as its long term stability in the oral environment, retention of the biopolymer coating on clinical application and, most importantly, the toxicity related to the oral tissues, must be carried out to justify its use as a befitting implantable biomaterial.

CONCLUSION

In the present study, we prepared two different types of Ti-nAg: one coated with regular AgNPs and the other coated with BP-AgNP. The SEM images of the microimplants showed that the AgNPs were favorably coated on the titanium alloy surface of both types of microimplants. The AgNPs varied in shape and size, with diameters in the range of 10 to 30 nm. EDS microanalysis confirmed a silver atomic % of 1.05 in the group coated with regular AgNPs and 21.2% in the group coated with BP-AgNP. XPS analysis confirmed the metallic state of silver. Disk diffusion tests showed that the Ti-BP-AgNP surface had remarkable antibacterial activity towards the oral bacteria *S. mutans*, *S. sanguinis*, and *A. actinomycetemcomitans*. These data suggest that Ti-BP-AgNP has excellent antibacterial properties, making it a promising implantable biomaterial.

REFERENCES

1. Le Guéhennec L, Soueidan A, Layrolle P, Amouriq Y. Surface treatments of titanium dental implants for rapid osseointegration. Dent Mater 2007;23:844-54.
2. Schierholz JM, Beuth J. Implant infections: a haven for opportunistic bacteria. J Hosp Infect 2001; 49:87-93.
3. Quirynen M, De Soete M, van Steenberghe D. Infectious risks for oral implants: a review of the literature. Clin Oral Implants Res 2002;13:1-19.
4. Zitzmann NU, Berglundh T, Ericsson I, Lindhe J. Spontaneous progression of experimentally induced periimplantitis. J Clin Periodontol 2004;31:845-9.
5. Ericsson I, Berglundh T, Marinello C, Liljenberg B, Lindhe J. Long-standing plaque and gingivitis at implants and teeth in the dog. Clin Oral Implants Res 1992;3:99-103.
6. Lindhe J, Meyle J. Peri-implant diseases: Consensus Report of the Sixth European Workshop on Periodontology. J Clin Periodontol 2008;35(8 Suppl): 282-5.
7. Zitzmann NU, Berglundh T. Definition and prevalence of peri-implant diseases. J Clin Periodontol 2008;35(8 Suppl):286-91.
8. Wadström T. Molecular aspects of bacterial adhesion, colonization, and development of infections associated with biomaterials. J Invest Surg 1989;2:353-60.
9. Liao J, Anchun M, Zhu Z, Quan Y. Antibacterial titanium plate deposited by silver nanoparticles exhibits cell compatibility. Int J Nanomedicine 2010;5:337-42.
10. Meredith DO, Eschbach L, Riehle MO, Curtis AS, Richards RG. Microtopography of metal surfaces influence fibroblast growth by modifying cell shape, cytoskeleton, and adhesion. J Orthop Res 2007;25:1523-33.
11. Chang YY, Huang HL, Lai CH, Hsu JT, Shieh TM, Wu AY, et al. Analyses of antibacterial activity and cell compatibility of titanium coated with a Zr-C-N film. PLoS One 2013;8:e56771.
12. Oh EJ, Nguyen TDT, Lee SY, Jeon YM, Bae TS, Kim JG. Enhanced compatibility and initial stability of Ti6Al4V alloy orthodontic miniscrews subjected to anodization, cyclic precalcification, and heat treatment. Korean J Orthod 2014;44:246-53.
13. Cho YC, Cha JY, Hwang CJ, Park YC, Jung HS, Yu HS. Biologic stability of plasma ion-implanted miniscrews. Korean J Orthod 2013;43:120-6.
14. Crede CSF. Die verhutung der augenentzundung der neugeborenen (Ophthalmoblennorrhoea neonatorum) der haufigsten und wuchtigsten ursache der blindheit. Berlin: A. Hirschwald; 1884.

15. Buckley JJ, Lee AF, Olivic L, Wilsonb K. Hydroxyapatite supported antibacterial Ag3PO4 nanoparticles. J Mater Chem 2010;20:8056-63.
16. Ciobanu CS, Massuyeau F, Constantin LV, Predoi D. Structural and physical properties of antibacterial Ag-doped nano-hydroxyapatite synthesized at 100°C. Nanoscale Res Lett 2011;6:613.
17. Hotta M, Nakajima H, Yamamoto K, Aono M. Antibacterial temporary filling materials: the effect of adding various ratios of Ag-Zn-Zeolite. J Oral Rehabil 1998;25:485-9.
18. Kvítek L, Panáćek A, Soukupová J, Kolář M, Večeřová R, Prucek R, et al. Effect of surfactants and polymers on stability and antibacterial activity of silver nanoparticles (NPs). J Phys Chem C 2008; 112:5825-34.
19. Rusu VM, Ng CH, Wilke M, Tiersch B, Fratzl P, Peter MG. Size-controlled hydroxyapatite nanoparticles as self-organized organic-inorganic composite materials. Biomaterials 2005;26:5414-26.
20. Lim SI, Zhong CJ. Molecularly mediated processing and assembly of nanoparticles: exploring the interparticle interactions and structures. Acc Chem Res 2009;42:798-808.
21. Zheng J, Yu H, Li X, Zhang S. Enhanced photocatalytic activity of TiO2 nano-structured thin film with a silver hierarchical configuration. Appl Surf Sci 2008;254:1630-35.
22. Díaz M, Barba F, Miranda M, Guitián F, Torrecillas R, Moya JS. Synthesis and antimicrobial activity of a silver-hydroxyapatite nanocomposite. J Nanomater 2009;ID498505.
23. Moulder JF, Stickle WF, Sobol PE, Bomben KD. Handbook of X-ray photoelectron spectroscopy. Eden Prairie, MN: Perkin-Elmer Corp. 1992.
24. McQuillan JS, Infante HG, Stokes E, Shaw AM. Silver nanoparticle enhanced silver ion stress response in Escherichia coli K12. Nanotoxicology 2012;6:857-66.
25. Suresh AK, Pelletier DA, Wang W, Moon JW, Gu B, Mortensen NP, et al. Silver nanocrystallites: biofabrication using Shewanella oneidensis, and an evaluation of their comparative toxicity on gram-negative and gram-positive bacteria. Environ Sci Technol 2010;44:5210-5.
26. Xu H, Qu F, Xu H, Lai W, Andrew Wang Y, Aguilar ZP, et al. Role of reactive oxygen species in the antibacterial mechanism of silver nanoparticles on Escherichia coli O157:H7. Biometals 2012;25:45-53.
27. Taheri S, Vasilev K, Majewski P. Silver nanoparticles: synthesis, antimicrobial coatings, and applications for medical devices. Recent Pat Mater Sci 2015;8:166-75.
28. Ritz HL. Microbial population shifts in developing human dental plaque. Arch Oral Biol 1967;12:1561-8.
29. Sambhy V, MacBride MM, Peterson BR, Sen A. Silver bromide nanoparticle/polymer composites: dual action tunable antimicrobial materials. J Am Chem Soc 2006;128:9798-808.
30. Shi Z, Neoh KG, Kang ET. Surface-grafted viologen for precipitation of silver nanoparticles and their combined bactericidal activities. Langmuir 2004;20:6847-52.
31. Yuan W, Fu J, Su K, Ji J. Self-assembled chitosan/heparin multilayer film as a novel template for in situ synthesis of silver nanoparticles. Colloids Surf B Biointerfaces 2010;76:549-55.
32. Lischer S, Körner E, Balazs DJ, Shen D, Wick P, Grieder K, et al. Antibacterial burst-release from minimal Ag-containing plasma polymer coatings. J R Soc Interface 2011;8:1019-30.
33. Ho CH, Tobis J, Sprich C, Thomann R, Tiller JC. Nanoseparated polymeric networks with multiple antimicrobial properties. Adv Mater 2004;16:957-61.